

EPR spectra of caesium and potassium molybdates and tungstates

Yurii A. Koksharov, Alexey V. Avdei, Vladimir D. Dolzhenko and Yurii M. Kiselev*

Department of Chemistry, M. V. Lomonosov Moscow State University, 119992 Moscow, Russian Federation.
Fax: +7 095 939 0998; e-mail: kiselev@coord.chem.msu.ru

DOI: 10.1070/MC2005v015n02ABEH002067

Compounds prepared by the interaction of CsO_2 or KO_2 with WO_3 or MoO_3 were studied by EPR spectroscopy.

The structures of alkali metal tungstates and molybdates contain alkali metal cations and tetrahedral $\langle\text{WO}_4\rangle$ or $\langle\text{MoO}_4\rangle$ fragments, respectively.^{1,2} These compounds are of interest because they are convenient matrices in which metal ions, for example, rhodium, in high oxidation states can be stabilised. Thus, based on non-empirical quantum-mechanical calculations, Ermilov *et al.*³ assumed the possibility of the substitution of $\langle\text{Rh}^{\text{VI}}\text{O}_4\rangle$ for tetrahedral $\langle\text{W}^{\text{VI}}\text{O}_4\rangle$ fragments in tungstates with the scheelite structure.

Matrix systems can be produced with the use of a corresponding acid oxide and an alkali metal (potassium or caesium) superoxide. The latter is characterised by a high oxidising ability, and the synthesis can be performed at a relatively low temperature. This approach made it possible to prepare the $\text{Cs}_2\text{FeO}_4\cdot\text{Co}^{6+}$ matrix system⁴ with the cobalt ion in an extreme valence state.

Here, we report the results of an EPR study of compounds prepared by the interaction of CsO_2 or KO_2 with WO_3 or MoO_3 . Unexpectedly, we detected strong paramagnetic resonance signals in the resulting stoichiometric tungstates and molybdates, which exhibited unusual temperature dependence.

The samples of Cs_2MoO_4 , Cs_2WO_4 , K_2MoO_4 and K_2WO_4 were prepared by (i) the annealing of MoO_3 or WO_3 with CsO_2 in a flow of dry oxygen with the use of a silver or quartz boat or (ii) the heating of MoO_3 or WO_3 with CsO_2 or KO_2 in a nickel autoclave with a sapphire reactor insert with a silver cap.

The samples of MoO_3 and WO_3 were prepared by the annealing of ammonium paramolybdate and ammonium paratungstate, respectively, in a flow of oxygen at 600 °C. The samples of CsO_2 were prepared from caesium metal. Commercial KO_2 from Merck was used. The samples were prepared at various reagent ratios ($[\text{Mo}(\text{W})]:[\text{Cs}(\text{K})] = 1:2, 2:5$ and $1:3$), temperatures (400–600 °C) and exposures (20–70 h). The reactors were loaded and the products were removed in a dry box. The resulting samples of Cs_2MoO_4 , Cs_2WO_4 , K_2MoO_4 and K_2WO_4 were colourless, white-pink, light green or purple depending on the synthesis conditions.

The EPR spectra were measured on a Varian E4 spectrometer (X-band; operating frequency of ~9.15 GHz; 77–300 K) with an E-257 nitrogen flow cryostat. The temperature was measured

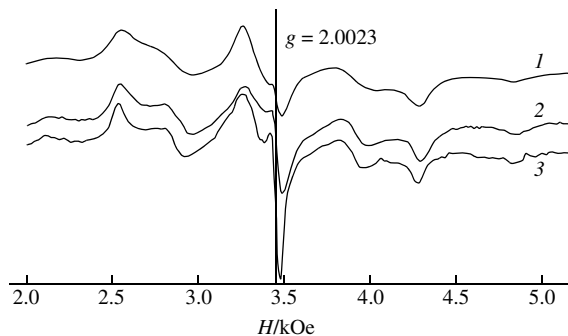


Figure 1 EPR spectra of Cs_2MoO_4 samples prepared by annealing in a flow of oxygen at (1) 873 K, (2) 763 K and (3) 623 K and $[\text{Mo}]:[\text{Cs}]$ molar ratio of 1:2.

to within 1 K using a 50 Ohm platinum resistor. The width (ΔH) and amplitude (A) of resonance lines were determined by the peak-to-peak method. The intensity of EPR signals was estimated from the equation $I = A\Delta H^2$.

The Raman spectra of solid samples were measured on a Nicolet Raman-950 Fourier spectrometer (Ge detector cooled with liquid nitrogen; spectral range to 4000 cm^{-1}). Published data⁵ were used for interpreting the Raman spectra. The powder X-ray diffraction patterns were obtained on a DRON-3M diffractometer ($\text{CuK}\alpha$ radiation, Ni filter).

As found by Raman spectroscopy, X-ray diffraction analysis and EPR spectroscopy, the starting oxides were free of foreign impurities, including paramagnetic impurities. The Raman spectra of the samples of Cs_2MoO_4 , K_2MoO_4 , Cs_2WO_4 and K_2WO_4 exhibited only bands due to the fundamental vibrations of $\langle\text{MoO}_4\rangle$ or $\langle\text{WO}_4\rangle$ tetrahedrons, respectively (Table 1). Powder X-ray diffraction data for all of the test samples at the molar ratio $[\text{Mo}(\text{W})]:[\text{Cs}(\text{K})] = 1:2$ indicate the occurrence of only a single phase, whose parameters are consistent with published data (Table 2).

Figure 1 demonstrates the EPR spectra of Cs_2MoO_4 prepared by the annealing of MoO_3 with CsO_2 in a flow of dry oxygen at different reaction temperatures. Note that all the EPR spectra of the molybdates and tungstates of caesium and potassium exhibited a relatively narrow component near $g \approx 2.00$. For

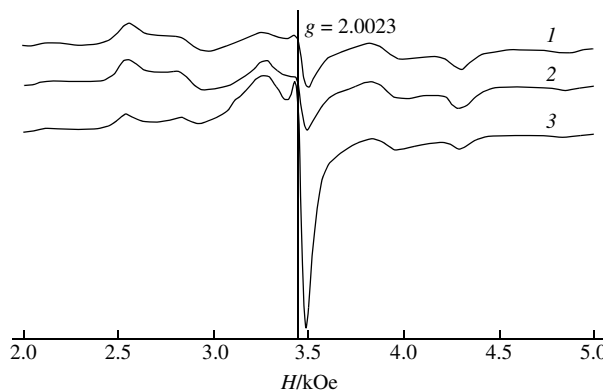


Figure 2 EPR spectra of Cs_2MoO_4 samples prepared by annealing in a flow of oxygen at 350 °C and the $[\text{Mo}]:[\text{Cs}]$ molar ratio of (1) 1:2, (2) 2:5 and (3) 1:3.

Table 1 Raman spectra of the molybdates and tungstates of potassium and caesium.

Sample	$\nu_1(A_1)/\text{cm}^{-1}$	$\nu_2(E)/\text{cm}^{-1}$	$\nu_3(F_2)/\text{cm}^{-1}$	$\nu_4(F_2)/\text{cm}^{-1}$
Cs_2MoO_4	885	320	839, 825	271
K_2MoO_4	890	320	854, 825	
K_2WO_4	923	320	854, 825	
Cs_2WO_4	923	323	838, 822	

Table 2 Unit cell parameters of the molybdates and tungstates of potassium and caesium.

Sample	$a/\text{\AA}$	$b/\text{\AA}$	$c/\text{\AA}$	$\beta/^\circ$	$V/\text{\AA}^3$
K_2MoO_4 (ref. 1)	12.345	6.087	7.535	115.73	509.3
K_2MoO_4 (expt.)	12.343(2)	6.082(1)	7.533(2)	115.66(1)	509.4(1)
K_2WO_4 (ref. 1)	12.380	6.117	7.554	115.96	514.4
K_2WO_4 (expt.)	12.379(8)	6.120(3)	7.549(4)	116.00(4)	514.0(3)
Cs_2MoO_4 (ref. 1)	6.551	11.586	8.499		645.2
Cs_2MoO_4 (expt.)	6.556(3)	11.587(5)	8.500(3)		645.8(4)
Cs_2WO_4 (ref. 1)	6.598	11.647	8.513		654.2
Cs_2WO_4 (expt.)	6.593(4)	11.649(5)	8.500(4)		652.8(7)

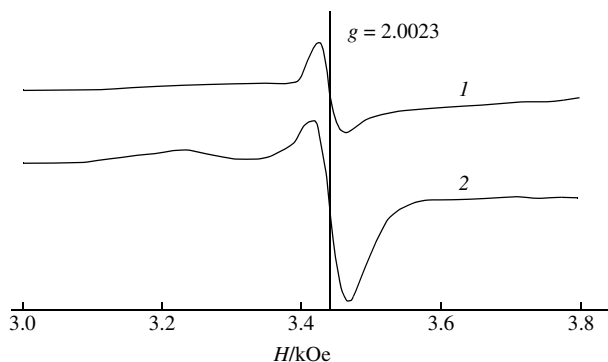


Figure 3 EPR spectra of Cs_2MoO_4 samples prepared in an autoclave at (1) 573 K and (2) 1163 K and $[\text{Mo}]:[\text{Cs}]$ molar ratio of 1:2.

caesium molybdate samples, the width of this line was 40–60 Oe, and its intensity decreased with synthesis temperature (Figure 1) and increased with superoxide concentration in the starting mixture (Figure 2). The other components of the EPR spectrum weakly depend on the synthesis temperature and the ratio Cs:Mo in the feed material.

Figure 3 demonstrates the EPR spectra of Cs_2MoO_4 prepared by another procedure (in an autoclave). A central line with $g \approx 2.00$ and a width of 40 Oe is predominant in these spectra. The intensity of the EPR spectrum increased as the synthesis temperature was decreased (Figure 3), however, to a lesser extent than in the samples prepared by annealing in a flow of oxygen (Figure 1).

Figure 4 demonstrates the EPR spectra of a Cs_2WO_4 sample prepared in an autoclave at 450 °C ($\tau = 40$ h). A very broad line ($\Delta H \approx 3$ kOe) is predominant in these spectra. In addition, there is a relatively narrow line ($\Delta H \approx 800$ Oe at 77 K) with a g -factor close to 1.988. As the temperature was decreased from room temperature to liquid nitrogen temperature, the width and amplitude of the narrow line noticeably increased (with reference to the broad line).

Figure 5 demonstrates the EPR spectra of a K_2MoO_4 sample prepared in an autoclave. As in the case of Cs_2WO_4 , the EPR spectra consist of two components: a very broad ($\Delta H \approx 3$ kOe) and a narrower component ($\Delta H \approx 200$ Oe). The narrow line has $g \approx 1.97$. At liquid nitrogen temperature, both components of the spectrum were noticeably broader than those at room temperature (Figure 5). It can be seen that, as the temperature was decreased from 100 to 77 K, the width of this component increased by a factor of 2.

Let us discuss the origin of EPR signals in the test samples. Stoichiometric M_2MoO_4 and M_2WO_4 ($\text{M} = \text{K}$ or Cs) should not contain paramagnetic centres; therefore, the EPR spectra detected are due to the occurrence of structure defects. Indeed, point defects containing pentavalent molybdenum occur in the molybdenum oxide MoO_3 .⁶ It is also well known^{7,8} that molybdenum bronzes, which also contain Mo^{V} , are formed by the introduction of hydrogen, alkali-metal and alkaline-earth cations into the structure of MoO_3 . Note that the EPR spectra obtained in this work are not typical of magnetically isolated Mo^{5+} and

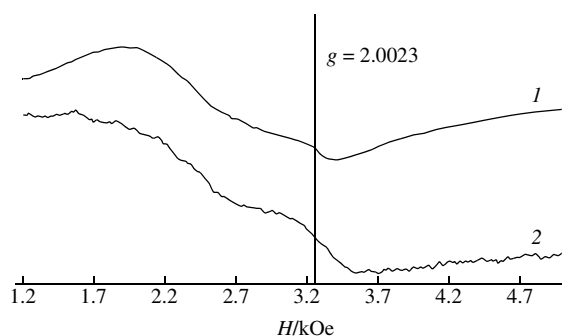


Figure 4 EPR spectra of a Cs_2WO_4 sample prepared in an autoclave ($T = 500$ °C; $[\text{W}]:[\text{Cs}] = 1:2$) measured at (1) 300 and (2) 77 K.

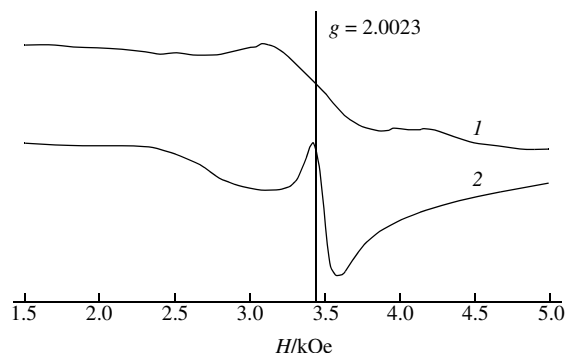


Figure 5 EPR spectra of a K_2MoO_4 sample prepared in an autoclave ($T = 400$ °C; $[\text{Mo}]:[\text{K}] = 1:2$) measured at (1) 300 and (2) 77 K.

W^{5+} . Indeed, the signal of Mo^{5+} is usually characterised⁹ by a hyperfine structure containing intense narrow lines from even isotopes with the average $g \approx 1.95$ and weaker lines from odd isotopes over the field region of about 100 Oe.

In addition to Mo^{5+} and W^{5+} , other paramagnetic defects and impurities can also produce EPR signals. Thus, the behaviour of the central EPR signal ($g \approx 2.001$, $\Delta H \approx 40$ –60 Oe) in caesium molybdate (the proportionality of the intensity of a spectral line to the amount of a superoxide in the starting mixture and a decrease in the intensity with increasing synthesis temperature) suggests that this signal is due to the superoxo group.

However, signals with $g \approx 1.97$ –1.99 in the samples of potassium molybdate and caesium tungstate are much wider (especially at low temperatures), and they may be attributed to Mo^{5+} and W^{5+} , respectively, arranged at crystal lattice defects. The absence of a hyperfine structure from the signals and a noticeable broadening with decreasing temperature can indicate the existence of magnetic clusters. It is important that similar EPR spectra were observed in molybdenum oxide nanoparticles.¹⁰

The EPR spectra of caesium molybdate also point to the possibility of defect clusterization because they exhibit a complex fine structure (Figures 1 and 2), which is characteristic of clusters with anisotropic exchange interactions.¹¹ At first approximation, the spectra in Figures 1 and 2 consist of seven relatively strong resonance lines. The central line (near $g \approx 2.0$) is likely the Mo^{5+} single-ion EPR spectrum with the fuzzy hyperfine structure. The other six lines could result, for example, from three-nuclear clusters of exchange-coupled Mo^{5+} ($4d^1$) ions. In case of ferromagnetic and only isotropic exchange interactions between spins-1/2 the ground state of such a cluster is characterized by the total spin $S_t = 3/2$ with three allowed EPR transitions ($-3/2 \rightarrow -1/2$; $-1/2 \rightarrow +1/2$ and $+1/2 \rightarrow +3/2$). Since the isotropic exchange interaction does not change the values of resonance fields, all these transitions should be observed near $g = 2.0$. However, the anisotropic exchange interaction can mix the states with $S_{tz} = \pm 1/2$; $\pm 3/2$ and provide the six transitions shifted from $g = 2.0$. Anisotropic exchange interactions could also be responsible (at least partially) for the disappearance of the EPR hyperfine structure.

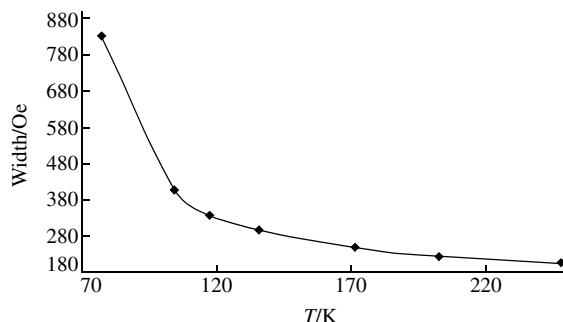


Figure 6 The temperature dependence of the width of an EPR line with $g \approx 1.974$ for a K_2MoO_4 sample prepared in an autoclave ($T = 400$ °C; $[\text{Mo}]:[\text{K}] = 1:2$).

In addition to the seven strongest lines, weaker resonances are visible in the EPR spectra, especially for the samples annealed at low temperatures (Figure 1). This fact points to the possible existence of clusters with four (or more) Mo^{5+} ions in Cs_2MoO_3 , prepared in a flow of oxygen. In other samples, in which the clusters probably become sufficiently large, the fine structure transforms into a single wide line (Figures 4 and 5) because of the dispersion of anisotropic exchange parameter values.

The EPR signals detected may be related to impurities such as iron. Indeed, the broadening of EPR signals with decreasing temperature, which was found in this work (Figure 6), is characteristic of magnetic nanoparticles of iron and iron oxides.¹² However, on cooling of magnetic nanoparticles, the EPR signal was downfield shifted, and we did not observe such a shift in our experiments. Note that, according to EPR data, the starting materials used for the synthesis of the samples were free of iron, as well as of other paramagnetic species.

Thus, we found that the synthesised samples of the molybdates and tungstates of potassium and caesium contained paramagnetic centres. It is probably that the properties of these centres are due to the presence of the exchange-coupled clusters of pentavalent molybdenum and tungsten. It is likely that there are various types of magnetic clusters, since the EPR spectra contain lines of different intensities, which depend on conditions of sample preparation. Single crystal experiments are expedient to effectively distinguish EPR spectra from different clusters.

This work was supported by the Russian Foundation for Basic Research (grant no. 02-03-33010).

References

- 1 F. X. Kools, A. S. Koster and G. D. Rieck, *Acta Crystallogr.*, 1970, **B26**, 1974.
- 2 V. I. Krivobock, G. M. Rozantsev and G. Ya. Samsonova, *Khimiya soedinenii molibdena i vol'frama (Chemistry of Molybdenum and Tungsten Compounds)*, Nauka, Novosibirsk, 1979, p. 119 (in Russian).
- 3 Yu. Ermilov, A. V. Avdei, E. G. Evtushenko, V. D. Dolzhenko and Yu. M. Kiselev, *Zh. Neorg. Khim.*, 2002, **47**, 1100 (*Russ. J. Inorg. Chem.*, 2002, **47**, 1008).
- 4 N. S. Kopelev, L. A. Kulikov, Yu. D. Perfiliev and Yu. M. Kiselev, *Zh. Neorg. Khim.*, 1995, **40**, 838 (*Russ. J. Inorg. Chem.*, 1995, **40**, 820).
- 5 K. Nakamoto, *Infra-red and Raman Spectra of Inorganic and Coordination Compounds*, Intersci Ltd., Singapore–Amsterdam–Toronto–New York, 1986.
- doi> 6 M. Labanowska, *Phys. Chem. Chem. Phys.*, 1999, **1**, 5385.
- 7 G. Bang and G. Sperlich, *Z. Physik*, 1975, **B22**, 1.
- 8 J. Dumas, B. Laayadi and R. Buder, *Phys. Rev.*, 1989, **B40**, 2968.
- 9 N. Marov and N. A. Kostromina, *EPR i YaMR v khimii koordinatsionnykh soedinenii (EPR and NMR in Coordination Compounds Chemistry)*, Nauka, Moscow, 1979 (in Russian).
- 10 N. A. Dhas and A. Gedanken, *J. Phys. Chem.*, 1997, **B101**, 9495.
- doi> 11 W. Bietsch, A. Mirea, T. Kamleiter, M. Weiss, U. S. Schubert, C. H. Weidl, C. Eschbaumer, I. Ovchinnikov and N. Domracheva, *Mol. Phys.*, 2002, **100**, 1957.
- doi> 12 Yu. A. Koksharov, S. P. Gubin, I. D. Kosobudsky, M. Beltran, Y. Khodorkovsky and A. M. Tishin, *J. Appl. Phys.*, 2000, **88**, 1587.

Received: 18th October 2004; Com. 04/2392